Fungal Biology 123 (2019) 59–65

Contents lists available at ScienceDirect

Fungal Biology

journal homepage: www.elsevier.com/locate/funbio

Mitochondrial alternative oxidase is determinant for growth and sporulation in the early diverging fungus *Blastocladiella emersonii*

Luis Alberto Luévano-Martínez [a, b], Camille C. Caldeira da Silva [a], Gianlucca G. Nicastro [a], Robert I. Schumacher [a], Alicia J. Kowaltowski [a], Suely L. Gomes [a, *]

[a] Departamento de Bioquímica, Instituto de Química, Universidade de São Paulo, São Paulo, São Paulo, Brazil
[b] Departamento de Parasitologia, Instituto de Ciências Biomédicas, Universidade de São Paulo, São Paulo, Brazil

ARTICLE INFO

Article history:
Received 25 June 2018
Received in revised form
31 October 2018
Accepted 8 November 2018
Available online 16 November 2018

Corresponding Editor: Jason Slot

Keywords:
AOX enzyme
Blastocladiomycete fungus
Life cycle control
Mitochondrial morphology
Respiratory activity

ABSTRACT

Blastocladiella emersonii is an early diverging fungus of the phylum Blastocladiomycota. During the life cycle of the fungus, mitochondrial morphology changes significantly, from a fragmented form in sessile vegetative cells to a fused network in motile zoospores. In this study, we visualize these morphological changes using a mitochondrial fluorescent probe and show that the respiratory capacity in zoospores is much higher than in vegetative cells, suggesting that mitochondrial morphology could be related to the differences in oxygen consumption. While studying the respiratory chain of the fungus, we observed an antimycin A and cyanide-insensitive, salicylhydroxamic (SHAM)-sensitive respiratory activity, indicative of a mitochondrial alternative oxidase (AOX) activity. The presence of AOX was confirmed by the finding of a *B. emersonii* cDNA encoding a putative AOX, and by detection of AOX protein in immunoblots. Inhibition of AOX activity by SHAM was found to significantly alter the capacity of the fungus to grow and sporulate, indicating that AOX participates in life cycle control in *B. emersonii*.

1. Introduction

Blastocladiella emersonii is a saprobic freshwater fungus that belongs to the phylum Blastocladiomycota (Blastocladiomycete class), located near the base of the fungal phylogenetic tree, close to the separation of fungi, animals and plants (James et al., 2006). The life cycle of *B. emersonii* is characterized by two distinct cell differentiation stages: germination and sporulation, during which a large number of morphological and biochemical changes occur (reviewed in Lovett, 1975). The cycle begins with the zoospore, a wall-less uninucleated non-growing motile cell that swims both towards light (Avelar et al., 2014) and nutrients (Lovett, 1975), subsisting for several hours on endogenous reserves. The germination stage starts once the zoospore reaches the appropriate environment. One of the first events observed during germination is the retraction of the zoospore single posterior flagellum, followed by the formation of a thin cell wall rich in chitin (Selitrennikoff et al., 1976). Germination also involves the release of ribosomes that are kept inactive in the nuclear cap, an organelle surrounding the nucleus (Lovett, 1963); the fragmentation or branching of the single giant cup-shaped mitochondrion, localized at the base of the flagellum, into numerous normal-sized mitochondria (Bromberg, 1974); and the formation of a germ tube that attaches the cell to the substrate (Barstow and Lovett, 1974). All these and other morphological changes give rise to the germling cell. This cell then enters the vegetative growth phase, which is characterized by intense nuclear division unaccompanied by cell division, generating a coenocyte. During growth, the germ tube elongates and begins to branch, forming a rhizoidal system, through which nutrients are absorbed.

At any time during vegetative growth, the sporulation stage can be induced by nutrient starvation. The first microscopic changes observed during this cell differentiation stage are: the formation of a basal septum, separating the body of the cell from the rhizoidal system, and the appearance of a papilla through which the zoospores will be released at the end of sporulation (Lessie and Lovett, 1968). Many other morphological changes occur during sporulation, including fusion of the numerous mitochondria, producing a giant mitochondrion located at the base of the zoospore flagellum

* Corresponding author. Departamento de Bioquímica, Instituto de Química, Universidade de São Paulo, Av. Prof. Lineu Prestes 748, São Paulo, São Paulo, 05508-000, Brazil. Fax: +55 11 3091 2186.
E-mail address: sulgomes@iq.usp.br (S.L. Gomes).

https://doi.org/10.1016/j.funbio.2018.11.005
1878-6146/

(Bromberg, 1974), cleavage of the cytoplasm around each nucleus and biogenesis of the flagellum, culminating with the production of the zoospores and their release to the medium. Nevertheless, little is known about the composition and role of the respiratory chain during these mitochondrial morphological changes. A search for components of the respiratory chain in *B. emersonii* cDNA expression libraries (http://blasto.iq.usp.br) and in the mitochondrial genome of the fungus revealed the presence of core subunits of the five electron transport chain and oxidative phosphorylation components in *B. emersonii* mitochondria, indicating that this organism presents a canonical respiratory chain (Ribichich et al., 2005; Tambor et al., 2008).

Mitochondrial alternative oxidase (AOX) is a ubiquitous respiratory enzyme found in plants, fungi, protists and some bacterial species. It provides an alternative electron transport pathway from coenzyme Q to oxygen, without proton pumping, therefore dissipating energy and decreasing ATP production. The investigation of the physiological role of this interesting enzyme has attracted the attention of researchers for a few decades, resulting in the discovery of a number of distinct functions in different organisms. For instance, AOX activity has been shown to be involved in cellular response to higher temperatures, deficiency of respiratory chain components (complex III or IV), nutrient deprivation and reactive oxygen species production, playing an important role in intracellular redox homeostasis (Hernandez et al., 2014; Joseph-Horne et al., 2001; Magnani et al., 2008; Martins et al., 2011; Rogov and Zvyagilskaya, 2015; Van Aken et al., 2009). However, to the best of our knowledge, no studies have been carried out with AOX in early diverging fungi such as *B. emersonii*, a fact that led us to investigate the presence and the role of this important enzyme in this fungus.

2. Materials and methods

2.1. Cell growth conditions

B. emersonii were maintained by harvesting zoospores released after incubation for 24 h at 22 ± 1 °C on PYG-agar growth medium (0.13 % peptone, 0.13 % yeast extract, and 0.3 % glucose in 1 % agar) in 100 mm Petri dishes. To obtain large quantities of zoospores or vegetative cells we inoculated 1×10^8 zoospores in 500 mL of defined DM4 liquid medium (Maia and Camargo, 1974) in a Fernbach flask, and incubated the culture for 16 h at 23 °C with moderate agitation. To collect the vegetative cells, a 45 mL aliquot (1×10^7 cells) was centrifuged at room temperature at 1000×*g* for 5 min, the pellet was washed with 150 mL of sporulation solution (SS: 1 mM Tris-maleate pH 6.8 containing 1 mM $CaCl_2$), and then the cells were resuspended in 5 mL SS for immediate use in oxygen consumption assays. To obtain the zoospores, the remaining culture was induced to sporulate by filtering the vegetative cells through nitex cloth and washing them with 1.5 L of SS. The cells are then resuspended in 400 mL SS and incubated at 27 °C with moderate agitation for about 3 h. After complete sporulation, the zoospores were collected by separating them from the empty vegetative cells (ghosts) by filtration through nitex cloth. The number of zoospores was determined by counting the cells in a Neubauer chamber, and zoospores were immediately used for oxygen consumption determination. To assay for the effects of AOX inhibition on germination, growth and sporulation of *B. emersonii*, zoospores (4×10^5 cells) obtained from PYG-agar growth were inoculated into tissue culture dishes (35 mm × 10 mm) containing 2 mL of DM4 liquid medium and incubated at 19 °C for 16 h. The solution containing SHAM (salicylhydroxamic acid dissolved in ddH_2O) was added to the medium according to each final concentration desired. Control cells were not treated with SHAM. To induce sporulation, vegetative cells grown in DM4 in the presence or absence of SHAM, adhered to the bottom of the dishes, were starved by withdrawal of the medium and washing the cells three times with 5 mL SS. The cells were then incubated for 6 h at room temperature with 2 mL SS. The cells were observed under a light microscope to visualize and count the different cell types. All experiments were done in triplicate, and the numbers shown in the results section are the average numbers determined from the triplicates. The relative sizes of the vegetative cells grown in the presence or absence of SHAM were estimated using the ImageJ program (Schneider et al., 2012), with at least 50 cells measured for each inhibitor concentration used.

2.2. Fluorescence and DIC microscopy assay

Fresh zoospores were harvested from PYG plates in HEPES buffer (HEPES 10 mM, $CaCl_2$ 1 mM, pH 7.0). Mitochondrial fluorescent probe DiOC6(3) (Invitrogen-Molecular Probes) was added to a final concentration of 0.1 μM and the cell suspension incubated for 30 min at room temperature. Alternatively, zoospores were incubated in PYG liquid medium for 120 min at 29 °C, to elicit differentiation into vegetative cells, and submitted to the same procedure to label mitochondria. Both populations were then fixed with paraformaldehyde (final concentration 4.0 %, in HEPES buffer). The suspensions were incubated overnight at 8 °C, to allow gentle decantation of the cells. The supernatant was discarded, and the cells resuspended in Glycerol 50 % in PBS, pH 8.0. Cell suspensions from both populations were mounted in microscopy slides with coverslips sealed with colorless nail polish. Cell images were produced in a Nikon Optiphot microscope with a dedicated digital camera, using a 100× oil immersion objective. For fluorescence, a dichroic filter (490 nm excitation, 530 nm emission) was employed, and the same fluorescent fields captured in differential interference contrast microscopy (Nomarski DIC). To enhance the fluorescent pictures, the digital images were submitted to blind deconvolution using a commercial software (Huygens Essential, version 17.10).

2.3. Respiratory activity

Cellular oxygen consumption was measured in an Oroboros high-resolution oxygraph at 30 °C. Cells (vegetative cells, 4×10^6/mL; zoospores, 1×10^7/mL) isolated from growth in liquid medium, under moderate agitation, were incubated in respiratory buffer (SS sporulation solution). After basal oxygen consumption determination, 4 μM antimycin A (a complex III inhibitor), 25 μM SHAM or 10 μM potassium cyanide (a complex IV inhibitor) were added to the incubation medium. In some experiments, 4 μM CCCP (a protonophore and uncoupler of oxidative phosphorylation) was included at the end of the experiment to determine the maximal respiratory capacity.

2.4. Carbonyl content quantification

Oxidative damage to proteins was determined by the carbonyl levels in total homogenates. Samples of vegetative cells and zoospores were treated with 20 mM 2,4-dinitrophenylhidrazine in 2 N HCl. Derivatized proteins were precipitated with 12 % trichloroacetic acid (TCA) and centrifuged for 10 min at 5000 g. Pellets were washed twice with cold ethanol: ethyl acetate (1:1). Pellets were washed with 20 mM phosphate buffer, pH 6.8. Samples were again precipitated with 12 % TCA. Pellets were dissolved in 6N guanidine hydrochloride. Carbonylated proteins were quantified spectrophotometrically at 460–470 nm using a molar extinction for hydrazine derivatives of 22 000 M^{-1} cm^{-1} (Levine et al., 1990).

2.5. Protein analysis and immunoanalysis

Zoospore and vegetative cell samples were lysed by mechanical disruption using glass beads for 5 min at maximal vortex capacity. Cell debris was eliminated by centrifugation at 1000×*g*. Protein was determined by the Bradford method. Proteins (50 μg per well) were resolved by standard SDS-PAGE. AOX and cytochrome *c* oxidase (subunit IV) expression were determined by western blotting. Antibodies against plant AOX (Agrisera, Vänäs, Cat No. AS04054) were used at a dilution of 1:200, and at 1:1000 dilution for cytochrome *c* oxidase subunit IV (Abcam, Cambridge, Cat No. ab16056). Secondary antibodies (Li-Cor Biosciences, Nebraska) were used at a dilution of 1:20 000. Proteins were visualized in an Odyssey fluorescence analyzer (Li-Cor Biosciences, Nebraska).

2.6. Statistical analysis

Three independent experiments were performed. Data were analyzed by two-way ANOVA using Origin 7.0. $p < 0.05$ was considered statistically significant. Data represent mean value ± SEM.

3. Results and discussion

3.1. Mitochondrial morphology changes drastically during B. emersonii life cycle

B. emersonii mitochondria, as mentioned above, undergo extensive morphological changes during the life cycle of the fungus (Bromberg, 1974). Zoospores (Fig. 1A), which constitute the motile stage of the cycle, have a unique giant cup-shaped mitochondrion located at the base of the posterior flagellum, as can be seen in Fig. 1B, that shows zoospores labelled with the mitochondrial fluorescent probe DiOC6(3), as described in Materials and Methods. Once the zoospores are exposed to nutrient medium they differentiate into vegetative cells, by retracting the single flagellum and growing a germ tube that will later give rise to a rhizoidal system (Fig. 1C). During this process the giant mitochondrion suffers fragmentation, giving rise to a large number of normal sized mitochondria that are distributed around the entire cell, as depicted in Fig. 1D. As vegetative cells are induced to sporulate by nutrient starvation, a series of morphological changes occur including the fusion of the several normal sized mitochondria to produce again the giant mitochondrion of the newly formed zoospore (not shown). However, no mitochondrial functional studies concerning these different mitochondria morphologies have been reported.

3.2. Mitochondrial oxygen consumption is higher in zoospores than in vegetative cells

In order to elucidate if mitochondrial morphological changes are accompanied by changes in mitochondrial functionality, we measured oxygen consumption in vegetative cells and zoospores obtained from liquid culture medium, under mild agitation, as described in Materials and Methods. As depicted in Fig. 2A, vegetative cells, which have several normal sized mitochondria (as shown in Fig. 1D), present a basal oxygen consumption of 2.6 nmol · (min · 10^7 cells)$^{-1}$. Oxygen consumption suffers a near 2-fold increase with a value of 4.7 nmol · (min · 10^7 cells)$^{-1}$ once vegetative cells transit to zoospores (Fig. 2B), which have a single giant cup-shaped mitochondrion, as shown in Fig. 1B. In addition, taking into account the differences in size of the cells and the corresponding amount of protein in them, oxygen consumption in zoospores is almost 5-fold higher than in vegetative cells, probably a necessity due to the fast swimming mode of the zoospores. As

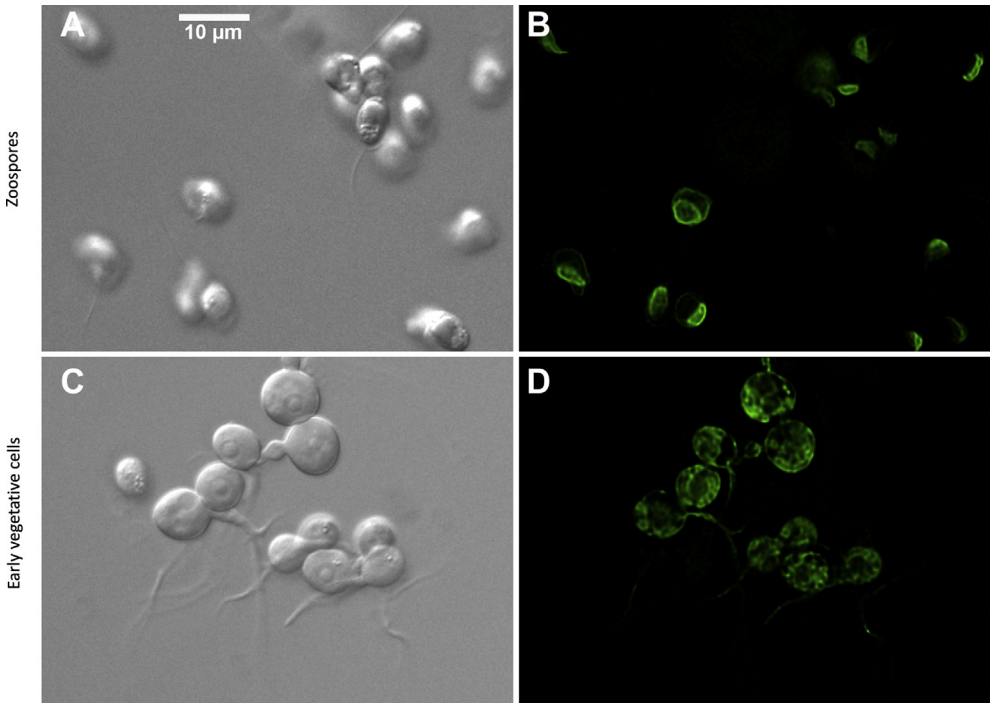

Fig. 1. Drastic mitochondrial morphology changes occur during the transition of zoospores to vegetative cells. Zoospores and early vegetative cells were labelled with the mitochondrial fluorescent probe DiOC6(3), which was added to the cell suspensions to a final concentration of 0.1 μM, as described in Materials and methods. Pannels (A) and (C) show the images of zoospores and early vegetative cells, respectively, obtained by differential interference contrast microscopy (Nomarski DIC), using a 100× oil immersion objective. Pannels (B) and (D) depict the mitochondria labelled with DiOC6(3) in zoospores and early vegetative cells, respectively. Images were obtained, as described in Material and methods, using a Nikon Optiphot microscope. Zoospore size varies from 7 to 9 microns.

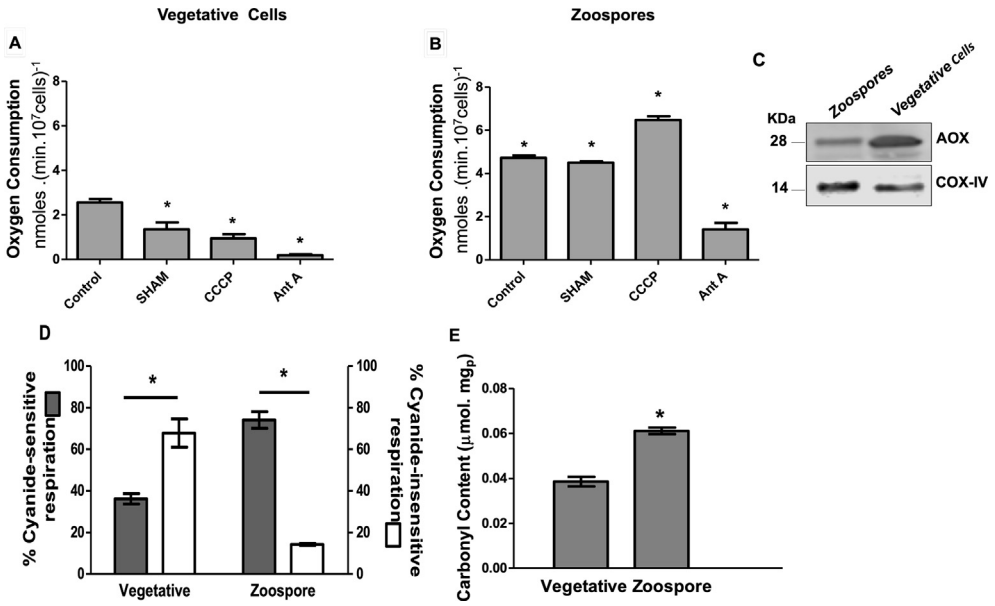

Fig. 2. Oxygen consumption is higher in zoospores than in vegetative cells and not inhibited by SHAM. Oxygen consumption rates were measured in respiratory buffer (SS-sporulation solution) for vegetative cells (A) or zoospores (B). After basal oxygen consumption determination, 25 μM SHAM, or 4 μM CCCP, or 4 μM antimycin A were included in the incubation medium. (C) Protein levels of AOX and COX-IV in cell extracts from vegetative and zoospore cells. Apparent molecular mass is indicated in kilodaltons. (D) COX (cyanide-sensitive) and AOX (cyanide-insensitive) dependent respiration in vegetative cells and zoospore. Oxygen consumption was measured in the presence of 10 μM KCN and 25 μM SHAM. (E) Oxidative damage to proteins. Carbonylated protein was measured in total homogenates. $^{*}p < 0.05$ respect to basal respiration.

both cell types were obtained in liquid medium under the same mild agitation, the oxygen concentration can be considered constant for both experiments, and the differences in oxygen consumption should be attributable to changes in cell physiology associated to the life cycle.

The higher oxygen consumption of zoospores versus vegetative cells seems to be consistent with the distinct mitochondrial morphology in these two cell types, as similar results were obtained during the analysis of mitochondrial morphology in yeast and many cultured mammalian cells, where interconnected mitochondrial networks were found to best meet the needs of respiratory-active cells, whereas small fragmented mitochondria were more prevalent in quiescent and respiratory-inactive cells (Westermann, 2012).

Additionally, when a mitochondrial uncoupler (CCCP) was added to the respiration medium in both cell types, a stimulating effect (1.5-fold) was observed in zoospores (Fig. 2B), which indicates that electron flow in the zoospore mitochondrion is coupled to ATP synthesis. On the other hand, in vegetative cells (Fig. 2A) CCCP did not affect oxygen consumption. These results indicate that the lower oxygen consumption observed in vegetative cells was diverted to other oxygen consuming processes, and not coupled to oxidative phosphorylation.

3.3. Mitochondrial oxygen consumption is inhibited by SHAM only in vegetative cells

As mentioned above, plants, fungi and some protists possess a mitochondrial alternative oxidase (AOX). This enzyme uses oxygen to directly oxidize the ubiquinol produced by upstream respiratory enzymes (Complex I and II). Thus, we decided to investigate if this enzyme was responsible for the variations in oxygen consumption observed between the cell stages. First, we asked if *B. emersonii* had such an enzyme through a search at the EST database of the fungus (http://blasto.iq.usp.br). We did find a cDNA encoding a putative mitochondrial alternative oxidase (clone BeE60H27F10), sequenced from a library constructed with RNA isolated from cells at the early stages of sporulation (30 min after induction) exposed to heat shock at 38 °C for 30 min (Georg and Gomes, 2007). The presence of AOX cDNA in a heat shock library is consistent with the report that AOX activity and transcript levels in fungi show a significant increase upon cell exposure to mildly higher temperatures (Honda et al., 2012).

To identify AOX activity, *B. emersonii* cells obtained from growth in liquid medium were incubated in the presence of the AOX inhibitor SHAM 25 μM final concentration resulting in a strong inhibition (46 % inhibition) in oxygen consumption in vegetative cells (Fig. 2A), whereas zoospore cells were practically unresponsive to this inhibitor (Fig. 2B). Antimycin A (an inhibitor of cytochrome *bc*1) was added at the end of the experiment to measure non-mitochondrial oxygen consumption. Residual oxygen consumption was ~1 % in vegetative cells and ~30 % in zoospore cells (Fig. 2A,B).

Altogether, these results suggest that respiratory activity is modulated during the life cycle of the fungus, with low respiration, in large part through AOX, in vegetative cells. Consistently, when relative protein levels of AOX and cytochrome *c* oxidase subunit IV (COX-IV) were measured, vegetative cells presented a 3-fold higher AOX level compared to the amount found in zoospores, whereas the levels of COX-IV were the same in both cell preparations (Fig. 2C). The observation that the relative amount of COX-IV does not change between zoospores and vegetative cells corroborate former work on *B. emersonii* mitochondrial function, which showed that cytochrome *c* oxidase activity was comparable in zoospores and vegetative cells (Horgen and Griffin, 1969). Moreover, when cyanide-sensitive respiration was measured (COX-dependent respiration) in both samples, a higher COX inhibition was observed in zoospore cells (Fig. 2D). On the other hand, cyanide-insensitive respiration was higher in vegetative cells (Fig. 2D), which is in line with the higher levels of the AOX protein observed in vegetative cells (Fig. 2C and respiration experiments in Fig. 2A,B). These data seem to indicate that zoospores, which have a high energy demand due to their necessity to swim for long periods of time in search of appropriate nutritional environments, have lower levels

of AOX. Indeed, zoospores would not benefit from an enzyme that, due to its capacity to bypass the proton-pumping cytochrome pathway, promotes significant energy dissipation. Interestingly, we observed a higher content of carbonylated protein in zoospores than in vegetative cells (Fig. 2E), indicating a higher oxidative damage to proteins in zoospores, which could be due to the higher respiratory rates observed in these cells (Fig. 2B), as well as a lower AOX protein level (Fig. 2C).

3.4. *Inhibition of alternative oxidase activity affects both growth and sporulation of* B. emersonii

As shown above, the inhibition of AOX activity in the presence of SHAM affects only the oxygen consumption of vegetative cells, and not the consumption of zoospores, consistent with the presence of higher levels (3-fold) of the AOX protein in vegetative cell extracts compared to zoospore extracts. In face of these results, we decided

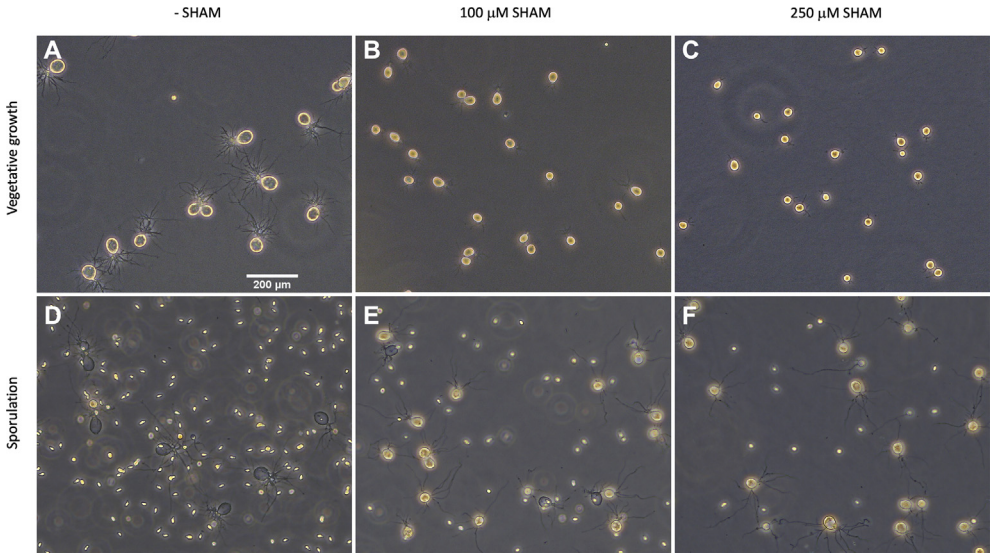

Fig. 3. Vegetative growth and sporulation are inhibited in cells treated with SHAM. The figure shows vegetative cells obtained by inoculation of zoospores in DM4 liquid medium in tissue culture dishes and incubation at 19 °C for 16 h, in the absence (A), or presence of 100 μM SHAM (B), or 250 μM SHAM (C). Vegetative cells in (A), (B) and (C) were then starved for nutrients and incubated in SS at room temperature for 6 h to induce sporulation. In (D), (E) and (F) we observed how the absence (D) or presence of 100 μM SHAM (E) or 250 μM SHAM (F) during growth affected the sporulation phase. The figure shows images of phase-contrast light microscopy.

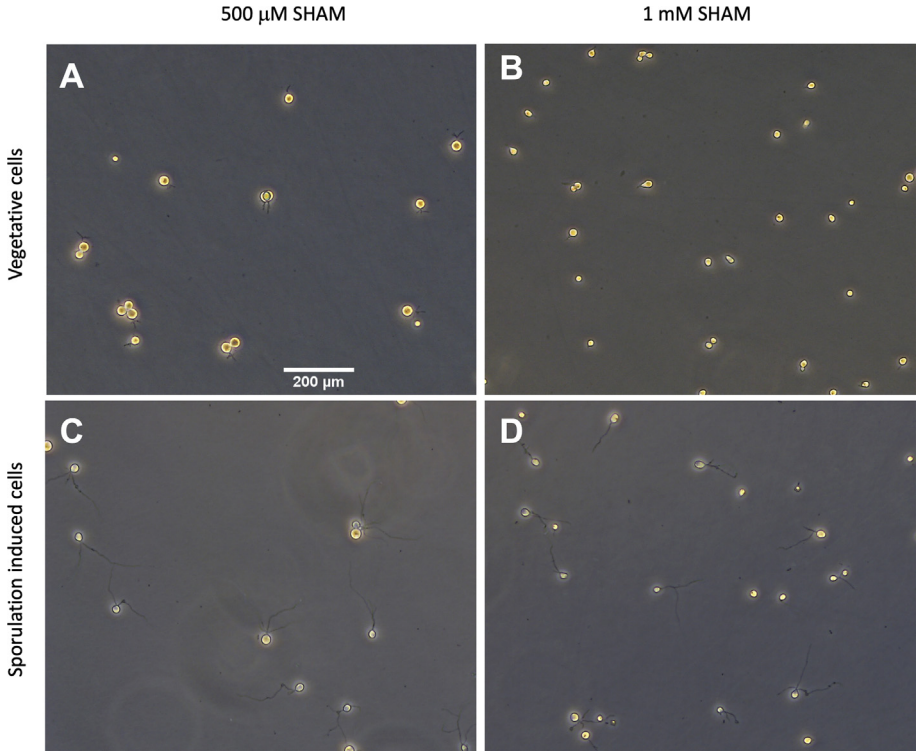

Fig. 4. Severe inhibition of vegetative growth and sporulation is observed at higher concentrations of SHAM. The figure depicts vegetative cells obtained from zoospores inoculated and incubated as described in Fig. 3, but in the presence of 500 μM (A) or 1 mM SHAM (B). Vegetative cells in (A) and (B) were then induced to sporulate as described in Fig. 3 and are depicted in (C) and (D), respectively.

to investigate if the presence of SHAM during *B. emersonii* life cycle could cause any physiological effect on the different cell types.

For that, we inoculated zoospores ($2 \cdot 10^5$ cells/mL) in tissue culture dishes containing 2 mL of defined DM4 medium and observed how they differentiate into germling cells as they germinate. In the presence of 100 μM or 250 μM SHAM (final concentration) zoospores presented a slight delay to differentiate into germling cells when compared to control cells in the absence of SHAM. This transition is easily observed under the light microscope, as zoospores stop swimming due to the retraction of the flagellum and grow a germ tube that attaches the cell to the substrate. These phenotypes appear in control cells (absence of SHAM) around 45 min after induction of germination at room temperature (Lovett, 1975). The germling cells then start to grow giving rise to vegetative cells, which reach a size 10–20 times larger than the zoospores after overnight incubation at 19 °C, as observed in Fig. 3A. However, when zoospore germination and vegetative growth occur in the presence of 100 μM SHAM (Fig. 3B) or 250 μM SHAM (Fig. 3C), vegetative cells reach much smaller sizes. Vegetative cells were determined to be 40 % smaller in the presence of 100 μM SHAM and 60 % smaller in the presence of 250 μM SHAM, when compared to the size of the cells grown in the absence of the AOX inhibitor (Fig. 3A). The cells were measured as described in Materials and methods. These results indicate a clear inhibitory effect of SHAM during growth.

We also analyzed the effect of SHAM on sporulation, which is induced by nutrient starvation of vegetative cells and culminates with the production and liberation of zoospores to the medium. As observed in Fig. 3D, control cells grown induced to sporulate in the absence of SHAM show complete sporulation, as after 5 h at room temperature 100 % of the sporulating cells are empty (ghosts) and a large number of zoospores ($2 \cdot 10^6$/mL) are observed (tiny cells seen among the ghosts of the sporulating cells). However, when vegetative cells were grown in the presence of 100 μM SHAM, less than 30 % of cells were able to complete sporulation, calculated as the percentage of empty vegetative cells (ghosts), and a lower number of zoospores ($3 \cdot 10^5$/mL) produced (Fig. 3E). In the presence of 250 μM SHAM, the inhibitory effect was even stronger, with less than 10 % of the cells completing the sporulation stage and very low number of zoospores ($4 \cdot 10^4$/mL) produced (Fig. 3F).

At higher concentrations of SHAM (500 μM or 1 mM, final concentration), the delay during germination was somewhat more pronounced, and the resulting vegetative cells were practically unable to grow. The cells reached sizes 70 % smaller in the presence of 500 μM SHAM and 75 % smaller in the presence of 1 mM SHAM (Fig. 4A,B, respectively), when compared to control cells grown in the absence of the AOX inhibitor (Fig. 3A). In addition, the sporulation stage was completely inhibited (Fig. 4C,D, respectively). No zoospores were detected and no empty cells (ghosts) were observed.

Nonetheless, all the effects observed in *B. emersonii* life cycle due to the presence of the Aox inhibitor SHAM are completely reversible. For instance, if vegetative cells were incubated overnight in the presence of 500 μM or 1 mM of SHAM, which inhibits their growth and sporulation, are washed and incubated with fresh defined medium DM4, these cells behave as if they were never exposed to SHAM. Vegetative cells show normal growth and are able to sporulate completely, producing normal zoospores, just as the control cells (Fig. 3A,D). The zoospores produced are in turn able to germinate and produce normal vegetative cells that can sporulate and produce new zoospores once again (not shown). These results confirm that the effects of SHAM are specific towards AOX.

Additionally, if SHAM (250 μM final concentration) was added only during induction of sporulation of vegetative cells grown in the absence of the AOX inhibitor (Fig. 5A), complete blockage of this cell differentiation stage was observed, with no empty cells (ghosts) or zoospores visualized (Fig. 5B). This result indicates that AOX has an essential role during this cell differentiation phase.

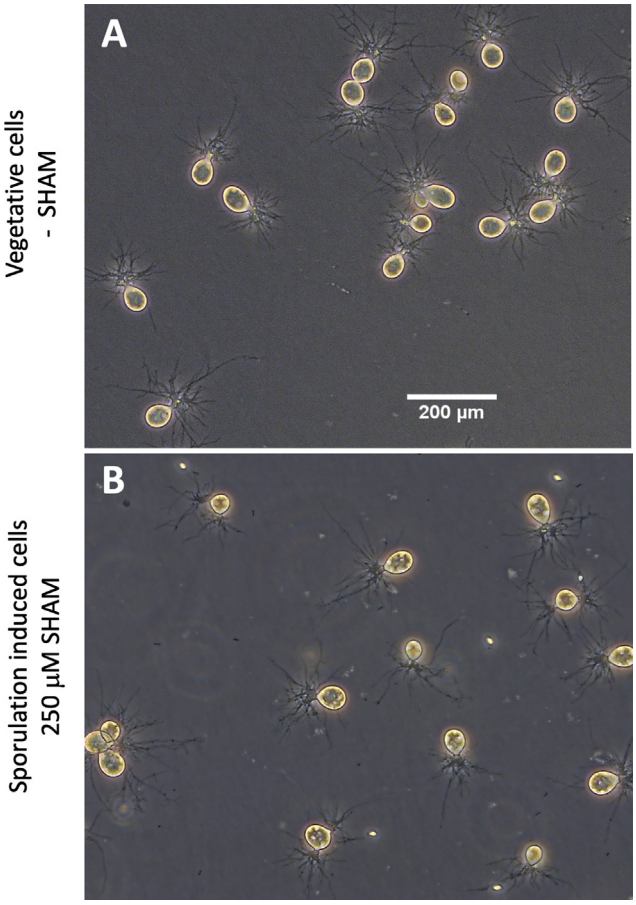

Fig. 5. SHAM inhibits sporulation of cells not exposed to the inhibitor during growth. The figure shows vegetative cells obtained from zoospores inoculated and incubated as described in Fig. 3 in the absence of SHAM (A), and then induced to sporulate in the presence of 250 μM SHAM (B).

4. Conclusions

In the present work we show that the respiratory capacity of the motile zoospores of the early diverging fungus *Blastocladiella emersoni*, which present a single giant cup-shaped mitochondrion, is much higher than in its sessile vegetative cells that carry a number of normal sized mitochondria. In addition, we observed an antimycin A-insensitive, salicylhydroxamic (SHAM)-sensitive respiratory activity in this fungus, indicative of a mitochondrial alternative oxidase activity (AOX). The presence of the enzyme was confirmed by the finding of a cDNA encoding a putative alternative oxidase in *B. emersonii* EST database (http://blasto.iq.usp.br), and by the immunodetection of the AOX protein using a specific anti-AOX antibody, with AOX protein levels being higher in vegetative cells than in zoospores. Our data also revealed that AOX activity is essential for vegetative growth and sporulation in *B. emersonii*, as the presence of SHAM inhibits both these stages of the fungus' life cycle in a dose-dependent manner. Even at low concentrations of SHAM (100 μM or 250 μM, final concentration), clear inhibitory effects are observed during growth and sporulation of the fungus. A possible explanation for the deleterious effects of AOX inhibition on

B. emersonii developmental cycle could be the increase in reactive oxygen species (ROS) production, causing subsequent cell damage. In growing cells, where genomic and mitochondrial DNA is being replicated, preventing ROS accumulation is quite important to protect against an increase in mutations, due to ROS mutagenic potential. The fundamental significance of AOX in alleviating or preventing oxidative stress has been described in a number of organisms, in fungi including yeasts, in algae and in plants (Rogov and Zvyagilskaya, 2015).

Conflicts of interest

The authors have no conflict of interest to declare for this research.

Acknowledgements

The authors wish to thank Luci D. Navarro, Sandra M. Fernandes and Edson Alves Gomes for expert technical assistance and Ana Paula Zen P. Fiore for her important help with the light microscopy. This work was supported by *Fundação de Amparo à Pesquisa do Estado de São Paulo* (FAPESP) grant to SLG (12/19960-1) and to AJK (13/07937-8) as part of the *CEPID de Processos Redox em Biomedicina (Redoxoma)*. SLG and AJK are partially supported by the Conselho *Nacional de Desenvolvimento Científico e Tecnológico* (CNPq). LALM is supported by a *Jovem Pesquisador* Fellowship from FAPESP (grant 2016/12999-0).

Appendix A. Supplementary data

Supplementary data to this article can be found online at https://doi.org/10.1016/j.funbio.2018.11.005.

References

Avelar, G.M., Schumacher, R.I., Zaini, P.A., Leonard, G., Richards, T.A., Gomes, S.L., 2014. A rhodopsin-guanylyl cyclase gene fusion functions in visual perception in a fungus. Curr. Biol. 24, 1234–1240.

Barstow, W.E., Lovett, J.S., 1974. Apical vesicles and microtubules in rhizoids of *Blastocladiella emersonii*: effects of actinomycin D and cycloheximide on development during germination. Protoplasma 82, 103–117.

Bromberg, R., 1974. Mitochondrial fragmentation during germination in *Blastocladiella emersonii*. Dev. Biol. 36, 187–194.

Georg, R.C., Gomes, S.L., 2007. Transcriptome analysis in response to heat shock and cadmium in the aquatic fungus *Blastocladiella emersonii*. Eukaryot. Cell 6, 1053–1062.

Hernandez, O., Araque, P., Tamayo, D., Restrepo, A., Herrera, S., Mcewen, J.G., Pelaez, C., Almeida, A., 2014. Alternative oxidase plays an important role in *Paracoccidioides brasiliensis* cellular homeostasis and morphological transition. Med. Mycol. 53, 205–214.

Honda, Y., Hattori, T., Kirimura, K., 2012. Visual expression analysis of the responses of the alternative gene (aox1) to heat shock, oxidative, and osmotic stresses in conidia of citric acid-producing *Aspergillus niger*. J. Biosci. Bioeng. 113, 338–342.

Horgen, P.A., Griffin, D.H., 1969. Cytochrome oxidase activity in *Blastocladiella emersonii*. Plant Physiol. 44, 1590–1593.

James, T.Y., Letcher, P.M., Longcore, J.E., Mozley-Standridge, S.E., Porter, D., Powell, M.J., Griffith, G.W., Vilgalys, R., 2006. A molecular phylogeny of the flagellated fungi (Chytridiomycota) and description of a new phylum (Blastocladiomycota). Mycologia 98, 860–871.

Joseph-Horne, T., Hollomon, D.W., Wood, P.M., 2001. Fungal respiration: a fusion of standard and alternative components. Biochim. Biophys. Acta 1504 (2–3), 179–195.

Lessie, P.E., Lovett, J.S., 1968. Ultrastructural changes during sporangium formation and zoospore differentiation in *Blastocladiella emersonii*. Am. J. Bot. 55, 220–236.

Levine, R.L., Garland, D., Oliver, C.N., Amici, A., Climent, I., Lenz, A.G., Ahn, B.W., Shaltiel, S., Stadtman, E.R., 1990. Determination of carbonyl content in oxidatively modified proteins. Methods Enzymol. 186, 464–478.

Lovett, J.S., 1963. Chemical and physical characterization of "nuclear caps" isolated from *Blastocladiella* zoospores. J. Bacteriol. 85, 1235–1245.

Lovett, J.S., 1975. Growth and differentiation of the water mold *Blastocladiella emersonii*: cytodifferentiation and the role of ribonucleic acid and protein synthesis. Bacteriol. Rev. 39, 345–404.

Magnani, T., Soriani, F.M., Martins, V. de P., Policarpo, A.C., Sorgi, C.A., Faccioli, L.H., Curti, C., Uyemura, S.A., 2008. Silencing of mitochondrial alternative oxidase gene of *Aspergillus fumigatus* enhances reactive oxygen species production and killing of the fungus by macrophages. J. Bioenergy Biomembr. 40, 631–636.

Maia, J.C.C., Camargo, E.P., 1974. c-AMP phosphodiesterase activity during growth and differentiation in *Blastocladiella emersonii*. Cell Differ. 1974, 147–155.

Martins, V.P., Dinamarco, T.M., Soriani, F.M., Tudella, V.G., Oliveira, S.C., Goldman, G.H., Curti, C., Uyemura, S.A., 2011. Involvement of an alternative oxidase in oxidative stress and mycelium-to-yeast differentiation in *Paracoccidioides brasiliensis*. Eukaryot. Cell 10, 237–248.

Ribichich, K.F., Salem-Izacc, S.M., Georg, R.C., Vêncio, R.Z.N., Navarro, L.D., Gomes, S.L., 2005. Gene discovery and expression profile analysis through sequencing of expressed sequence tags from different developmental stages of the chytridiomycete *Blastocladiella emersonii*. Eukaryot. Cell 4, 455–464.

Rogov, A.G., Zvyagilskaya, R.A., 2015. Physiological role of alternative oxidase (from yeasts to plants). Biochemistry (Mosc.) 80, 400–407.

Schneider, C.A., Rasband, W.S., Eliceiri, K.W., 2012. NIH Image to ImageJ: 25 years of image analysis. Nat. Methods 9, 671–675.

Selitrennikoff, C.P., Allin, D., Sonneborn, D.R., 1976. Chitin biosynthesis during *Blastocladiella* zoospore germination: evidence that the hexosamine biosynthetic pathway is post-translationally activated during cell differentiation. Proc. Natl. Acad. Sci. USA 73, 534–538.

Tambor, J.H.M., Ribichich, K.F., Gomes, S.L., 2008. The mitochondrial view of *Blastocladiella emersonii*. Gene 424, 33–39.

Van Aken, O., Giraud, E., Clifton, R., Whelan, J., 2009. Alternative oxidase: a target and regulator of stress responses. Physiol. Plant 137, 354–361.

Westermann, B., 2012. Bioenergetic role of mitochondrial fusion and fission. Biochim. Biophys. Acta 1817, 1833–1838.